Probabilistic Intensity Mapping in MRI Image Registration

ALEXEI MANSO CORRÊA MACHADO[1], MARIO FERNANDO MONTENEGRO CAMPOS[2], JAMES GEE[3]

[1]Pontifícia Universidade Católica de Minas Gerais- Depto. de Ciência da Computação
Av. Dom José Gaspar 500, Belo Horizonte, MG, 30535-610, Brazil - alexei@pucminas.br
[2]Universidade Federal de Minas Gerais - Depto. de Ciência da Computação
Caixa Postal 702, Belo Horizonte, MG, 30161-970, Brazil - mario@dcc.ufmg.br
[3]University of Pennsylvania - Department of Radiology
3400 Spruce Street, Philadelphia, PA, 19104, USA - gee@grip.cis.upenn.edu

Abstract. In this work, we present a method which is able to relate different MR sensors with respect to intensity distortions in the output images. For the important problem of image registration, the method makes possible a principled approach to likelihood modeling or the construction of similarity metrics. Likelihood models can be used as prior knowledge of the relationship between intensities in both images, providing a fundamental information resource for image registration. A poor model of the intensity mapping for the image pair to be matched may lead to false matches, regardless of the prior morphological constraints assumed and will bias all subsequent analyses. A formal analysis of robustness under different kinds of noise is also provided and the findings compared to other relevant similarity metrics. Experiments are controlled based on the application of synthetic spatial and intensity deformations that guarantee a fiducial basis for comparison.

1 Introduction

During the past decades, advances in the technology of medical image processing has been responsible for a revolution in the field of non-invasive diagnosis. Nowadays, the use of techniques such as magnetic resonance imaging (MRI) is broadly disseminated even in underdeveloped countries and constitutes a great benefit to mankind. Although this technology is able to provide detailed information regarding human anatomy, the same cannot be asserted of techniques used to interpret and classify these data. Images are only two-dimensional signals unless symbolic information regarding to what is being imaged can be extracted and this constitutes the main challenge of medical imaging research.

Different MRI sensors may provide distinct intensities for the same tissue, due to differences in the magnetic field, noise, positioning and other variables related to the acquisition step. The purpose of this work is to propose a method which is able to relate different sensors with respect to intensity distortions or *artifacts* in the imaging process and support robust data analysis. The importance of the proposed method is manifold. It is a tool to model the sensors used in the acquisition step, whose behavior must be better understood in order to improve subsequent data processing. For the important problem of image registration, the method should also make possible a principled approach to likelihood modeling or the construction of similarity metrics. Likelihood models can be used as prior knowledge of the relationship between intensities in both images, providing a fundamental information resource for image registration. A poor model of the intensity mapping for the image pair to be matched may lead to false matches, regardless of the prior morphological constraints assumed and will bias all subsequent analyses.

The first step in the process of image registration is the acquisition of the original images, which are obtained by a sensor (e.g. MRI scanner) and stored in digital format as an array of two-dimensional slices. One of the images is used as an *atlas* or *reference* I_R which will be deformed to match each of the *test* subjects I_T in the study. Since the reference and test volumes may be misaligned with respect to one another, due to differences in head positioning inside the scanner, a *global registration* step consisting of rigid transformations (translation and rotation) is applied in order to approximately register corresponding features and aid the warping process.

The *local registration* step or *warping* is responsible for the non-rigid deformation of the reference image onto the subject's image. Image volumes may be described as continuous media to which a constitutive model will be prescribed. The *linear elasticity* model proposed by Broit and Bajcsy [1], in which the image is deformed as an elastic body, is the most commonly used. The model guarantees smoothness to the deformation, so that neighboring structures in the reference image will be matched to neighboring structures in the subject's image, preserving the gross anatomy common to the majority of individuals in the population. The output of the local registration step is a set of *spatial mappings* or *displacement fields*, one for each subject, which describes the point-wise deformation that was needed to match I_R to I_T.

0-7695-0878-2/00 $10.00 © 2000 IEEE

The results of image registration essentially depend on two aspects: an appropriate model of deformation and an intensity mapping strategy that provides a similarity measure to evaluates each candidate displacement field. Many similarity measures or metrics, such as the cross-correlation [3], mutual information [14, 9, 10] and histogram-matching approaches [8] have been used in image registration. These metrics provide a measure of similarity between a region in the reference image and the corresponding region in the test image, which were mapped by means of the displacement field resulting from warping. Due to the fact that these measures provide scalar values rather than a distribution for the intensity mapping between the two spectra, intensity artifacts may not be properly accounted for and favor incorrect deformations.

In this work, we propose a novel approach to address the evaluation of similarity for a candidate deformation. The method computes a probability distribution that gives, for each intensity in the reference image, the likelihood that it corresponds to an intensity of the test image spectrum. The distribution can be used to measure similarity, but essentially provides more complex information that can be used as prior knowledge in the local registration process, for matching other images that were acquired with the same sensor. The method determines a likelihood model for each sensor, accounting for inherent intensity distortions and therefore increasing the robustness of the warping process with respect to the influence of strong artifacts.

2 Methods

The choice of candidate points for matching relies on using a model that describes the likelihood of correspondence between the intensity of a voxel at position $\mathbf{p}$ in the test image, given that the intensity of a voxel at position $\mathbf{q}$ in reference image has been observed. If we know the model that relates both MRI scanners, we can choose the points in the the test image that are most likely to fit the model description. The best candidates can be evaluated by an optimization algorithm which finds the configuration that minimizes the overall displacement of points, according to morphological constraints [5].

2.1 Likelihood Models

The relationship between the variables of the intensity mapping problem in image matching can be better understood when they are displayed as a causal model [11]. The model in Fig. 1 specifies that the intensity of each voxel in the image depends on the tissue mixture within the voxel and on the voxel's position within the scanner volume. Due to sampling in the acquisition step, a voxel may be composed of a mixture of tissues, which will result on a wide variation of intensities shown for each one. Variable V can be interpreted as the intensity output that is due exclusively to the tissue mixture M of the voxel being inspected. It is known, however, that the actual intensity output is influenced by the position in which the voxel is placed within the scanner volume. The model shows that the same voxel composed of a fixed mixture M of different tissue types may produce different intensities T and R when placed in different positions or scanners P and Q, respectively. Taking output intensity T as an example, its value would be equal to V if only the tissue were taken into account. However, since it is placed at position P, its value is also influenced by the sensor characteristics.

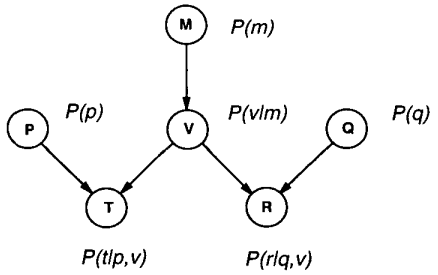

Figure 1: A causal network for the intensity mapping problem with the associated probability distributions.

Since the intensity variable T is influenced by the voxel's intensity output V which is due to tissue mixture and the position P at which the voxel is placed, the probability that it assumes a value t is *conditioned* on the values of V and P. This quantitative information is denoted as $P(t|v, \mathbf{p})$, which represents an *observation model*. We can state the same for intensity observations in the reference image for the matching problem, where $P(r|v, \mathbf{q})$ is the conditional probability that a voxel presenting intensity v, due to tissue composition, will result on intensity r when placed at position $\mathbf{q}$.

During the matching process, for each voxel positioned at $\mathbf{q}$ of known intensity r, the aim is to find its corresponding voxel in image T. To do so, it is necessary to determine how likely it is for a voxel with intensity t placed at candidate position $\mathbf{p}$ to contain the same tissue mixture that voxel $\mathbf{q}$ is composed of. The problem can be stated as the determination of the probability $P(t|\mathbf{p}, r, \mathbf{q})$. The values $\mathbf{p}$, r and $\mathbf{q}$ are *evidences* that change the prior degree of belief on the values of T. Conditioning $P(t|\mathbf{p}, r, \mathbf{q})$ on the exhaustive continuous range of output intensities values due to tissue mixture, we have that

$$P(t|\mathbf{p}, r, \mathbf{q}) = \int_{-\infty}^{+\infty} P(t|\mathbf{p}, r, \mathbf{q}, v) P(v|\mathbf{p}, r, \mathbf{q}) dv. \quad (1)$$

In addition to the dependencies between the variables, the causal model in Fig. 1 also represents the conditional

independent relationships between them. In fact, given that intensity value v is known, the information about variables R and Q does not contribute to our belief on the value of T. In other words, T is *conditionally independent* from R and Q given that V is known. Moreover, since T is unknown, it causes the variable V to be independent of P. These independencies can be denoted as $P(t|\mathbf{p}, r, \mathbf{q}, v) = P(t|\mathbf{p}, v)$ and $P(v|\mathbf{p}, r, \mathbf{q}) = P(v|r, \mathbf{q})$, which together with Eq. 1 leads to

$$P(t|\mathbf{p}, r, \mathbf{q}) = \int_{-\infty}^{+\infty} P(t|\mathbf{p}, v)P(v|r, \mathbf{q})dv. \quad (2)$$

Using Bayes' formula, we have that

$$P(v|r, \mathbf{q}) = P(r, \mathbf{q}|v)P(v)/P(r, \mathbf{q}),$$

which together with Eq. 2 leads to

$$P(t|\mathbf{p}, r, \mathbf{q}) = \frac{1}{P(r, \mathbf{q})} \int_{-\infty}^{+\infty} P(t|\mathbf{p}, v)P(r, \mathbf{q}|v)P(v)dv. \quad (3)$$

Using the definition of conditional probability we have that $P(r, \mathbf{q}|v) = P(r|\mathbf{q}, v)P(\mathbf{q}|v)$, where $P(\mathbf{q}|v) = P(\mathbf{q})$, since Q is independent from V when variable R is unknown. From Eq. 3, it follows that

$$P(t|\mathbf{p}, r, \mathbf{q}) = \frac{P(\mathbf{q})}{P(r, \mathbf{q})} \int_{-\infty}^{+\infty} P(t|\mathbf{p}, v)P(r|\mathbf{q}, v)P(v)dv. \quad (4)$$

Finally, conditioning $P(v)$ on the continuous exhaustive range of tissue mixture values, we have that

$$P(v) = \int_{-\infty}^{+\infty} P(v|m)P(m)dm,$$

which together with Eq. 4 leads to

$$P(t|\mathbf{p}, r, \mathbf{q}) = \frac{P(\mathbf{q})}{P(r, \mathbf{q})} \int_{-\infty}^{+\infty} P(t|\mathbf{p}, v)P(r|\mathbf{q}, v) \int_{-\infty}^{+\infty} P(v|m)P(m)dmdv. \quad (5)$$

Eq. 5 shows that $P(t|\mathbf{p}, r, \mathbf{q})$ is an average of the product of the observation models, for each partial volume tissue mixture, weighted by its *a priori* probability.

In order to use Eq. 5 as a similarity measure to image registration, the observation models $P(t|\mathbf{p}, v)$ and $P(r|\mathbf{q}, v)$ must be specified. Based on the characteristics of MRI sensors [4], the probability distribution functions can be model as Gaussian distributions. This model is appropriate for MRI images, but should be replaced with the relevant distribution in other imaging situations. Since the probabilities are represented in practice by tables, our method is applicable to any class of distributions. Assuming Gaussian distributions for the observation models, Eq. 5 becomes

$$P(t|\mathbf{p}, r, \mathbf{q}) = \alpha \int_{-\infty}^{+\infty} \exp\left(-\frac{(t - \mu_{T\mathbf{p}v})^2}{2\sigma_T^2}\right) \exp\left(-\frac{(r - \mu_{R\mathbf{q}v})^2}{2\sigma_R^2}\right) \int_{-\infty}^{+\infty} P(v|m)P(m)dmdv, \quad (6)$$

where α represents the constant terms that do not affect the degree of belief on t, given the evidence, and is such that the exhaustive sum of $P(t|\mathbf{p}, r, \mathbf{q})$ over all possible values of t is the unity. The variances σ_T^2 and σ_R^2 can be assumed spatially constant and are easily determined from the image background, for each sensor [4]. The means $\mu_{T\mathbf{p}v}$, $\mu_{R\mathbf{q}v}$ express the expected output intensity for a voxel being imaged at each position of sensors T and R.

2.2 Robustness analysis

The choice of which measure to use as a similarity function in the elastic matching model should take into account the behavior of the measure under position-dependent noise. As seen, the output intensity value does not depend exclusively on the tissue being imaged, but is in fact distorted by the variations of the magnetic field inside the scanner, resulting in image artifacts. While it is proven that the cross-correlation, mutual information and histogram matching approaches to similarity measurements are invariant only to constant noise [7], we show that the likelihood model measure is invariant to any sort of position-dependent noise:

Theorem 2.1 *The likelihood model measure is invariant to generic additive noise.*

PROOF — *The hypothesis is true if*

$$P(t|\mathbf{p}, r, \mathbf{q}) = \hat{P}(\hat{t}|\mathbf{p}, r, \mathbf{q}), \quad (7)$$

where $\hat{t}$ is intensity t added by a noise K which is function of $\mathbf{p}$:

$$\hat{t} = t + K(\mathbf{p}). \quad (8)$$

Since K is a function of position, the mean intensity value $\mu_{T\mathbf{p}v}$ will also be added by $K(\mathbf{p})$, resulting on

$$\hat{\mu}_{T\mathbf{p}v} = \mu_{T\mathbf{p}v} + K(\mathbf{p}). \quad (9)$$

The additive noise $K(\mathbf{p})$ does not affect variance σ_T^2:

$$\hat{\sigma}_T^2 = \sigma_T^2. \quad (10)$$

From Eq. 6 to 10, it follows that

$$\alpha \int_{-\infty}^{+\infty} \exp\left(-\frac{(t - \mu_{T\mathbf{p}v})^2}{2\sigma_T^2}\right) \exp\left(-\frac{(r - \mu_{R\mathbf{q}v})^2}{2\sigma_R^2}\right) \int_{-\infty}^{+\infty} P(v|m)P(m)dmdv = \alpha \int_{-\infty}^{+\infty} \exp\left(-\frac{(t + K(\mathbf{p}) - \mu_{T\mathbf{p}v} - K(\mathbf{p}))^2}{2\sigma_T^2}\right) \exp\left(-\frac{(r - \mu_{R\mathbf{q}v})^2}{2\sigma_R^2}\right) \int_{-\infty}^{+\infty} P(v|m)P(m)dmdv,$$

which completes the proof.

Theorem 2.2 *The likelihood model measure is invariant to generic multiplicative position-dependent noise.*

PROOF — *The hypothesis is true if and only if*

$$P(t|\mathbf{p}, r, \mathbf{q}) = \hat{P}(\hat{t}|\mathbf{p}, r, \mathbf{q}), \tag{11}$$

where $\hat{t}$ is intensity t multiplied by a positive noise K which is function of $\mathbf{p}$:

$$\hat{t} = K(\mathbf{p})t. \tag{12}$$

Since K is a function of position, the mean intensity value $\mu_{T\mathbf{p}v}$ will also be multiplied by $K(\mathbf{p})$, resulting on

$$\hat{\mu}_{T\mathbf{p}v} = K(\mathbf{p})\mu_{T\mathbf{p}v}. \tag{13}$$

The multiplicative noise $K(\mathbf{p})$ affects variance σ_T^2 in that it is multiplied by the square of noise K:

$$\hat{\sigma}_T^2 = K(\mathbf{p})^2\sigma_T^2. \tag{14}$$

From Eq. 6 and 11 to 14, it follows that

$$\alpha \int_{-\infty}^{+\infty} \exp\left(-\frac{(t-\mu_{T\mathbf{p}v})^2}{2\sigma_T^2}\right) \exp\left(-\frac{(r-\mu_{R\mathbf{q}v})^2}{2\sigma_R^2}\right) \int_{-\infty}^{+\infty} P(v|m)P(m)dmdv =$$

$$\hat{\alpha} \int_{-\infty}^{+\infty} \exp\left(-\frac{(K(\mathbf{p})t - K(\mathbf{p})\mu_{T\mathbf{p}v})^2}{2K(\mathbf{p})^2\sigma_T^2}\right) \exp\left(-\frac{(r-\mu_{R\mathbf{q}v})^2}{2\sigma_R^2}\right) \int_{-\infty}^{+\infty} P(v|m)P(m)dmdv,$$

which completes the proof.

2.3 Implementation

In the likelihood model described in Eq. 6, the means $\mu_{T\mathbf{p}v}$ and $\mu_{R\mathbf{q}v}$ have special meaning. Taking sensor T as an example, the mean $\mu_{T\mathbf{p}v}$ is the expected output intensity for a voxel being imaged at position $\mathbf{p}$, which would give output v if only its tissue composition would influence intensity. Variable V could be thought as the output of an "ideal sensor" which is able to precisely determine the output intensity based exclusively on the tissue composition of the voxel. Since no real sensor is able of producing perfect output, the mean values can be estimated in the discrete domain, based on a set of images segmented into tissue types. The rationale for the method is closely related to the use of deformable atlases. In image registration, a reference image called the *atlas* is deformed to match other images in order to serve as a basis for shape comparison. In the proposed method, a specific observation model will be used as a *observation model template* that will be matched to the observation models with which the reference and test images were acquired. The connection among the observation model template, the reference and test observation models can be better understood with the aid of Fig. 1. The reference observation model is determined by the probability function $P(r|\mathbf{q}, v)$ relating variable R to variables Q and V. In a similar way, the test observation model is determined by the probability function $P(t|\mathbf{p}, v)$ relating variable T to variables P and V. The variable connecting these two probability functions is V, which is influenced by tissue composition. The observation model template is described as a probability function $\mathbf{P}(v|m)$ which gives the likelihood that each tissue mixture m will produce output intensity v. While the reference and test observation models depend on position (variables Q and P, respectively), the observation model template is determined only by the tissue mixtures being imaged. We shall prove that any probability function $\mathbf{P}(v|m)$ can be used as an observation model template.

The process of estimating the mean values will be presented taking observation model T as an example. The value of $\mu_{T\mathbf{p}v}$ can be approximated by considering the intensity values that each tissue assumes in the neighborhood of position $\mathbf{p}$. The region of the test image around position $\mathbf{p}$ will be called A. The first step is to compute the intensity IH_T and tissue TH_T histograms in region A based on the gray-level and segmented images, respectively. The dimensions of A are parameters to be determined experimentally. If the area is too large, it may encompass strong position-dependent intensity variation; if it is too small, the histograms will be of reduced statistical confidence. In order to assure a smooth distribution and ameliorate the effect of the smaller region dimension, the intensity histogram should be smoothed with the aid of a kernel function [13] (e.g. a Gaussian with small variance).

The role of the tissue histogram is to enable the calculation of the expected intensity histogram in the observation model template. If the tissue distribution TH_T for region A in the test image is known and the observation model template $P(v|m)$ gives the expected distribution of intensity v for tissue m, the expected intensity histogram for the observation model template, $IH_{ET}(v)$, can be computed as

$$IH_{ET}(v) = \int_{-\infty}^{+\infty} P(v|m)TH_T(m)dm, \tag{15}$$

where $TH_T(m)$ is the *a priori* probability distribution $P(m)$ for the tissue mixture m. In practice, the integral at Eq. 15 is replaced by a sum, since segmented images are discrete valued and usually contain just three major tissues types: cerebrospinal fluid, gray and white matter.

The final step in determining the mean values is matching the expected histogram IH_{ET} computed by Eq. 15 to the test intensity histogram IH_T. For each intensity v, the corresponding matched intensity in the histogram IH_T is

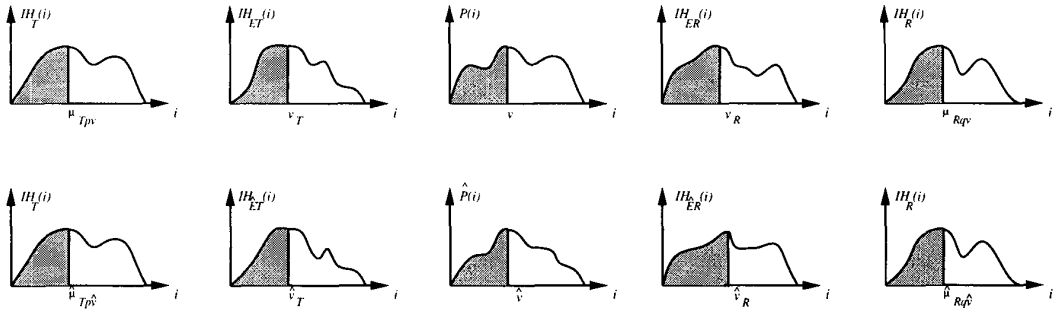

Figure 2: The relationship between the cumulative areas in the histogram matching process. The gray areas shown in the histograms have the same value.

the mean value $\mu_{T\mathbf{p}v}$ for the region around $\mathbf{p}$. The mean values can be computed incrementally by satisfying the following relationship:

$$\frac{\int_{-\infty}^{\mu_{T\mathbf{p}v}} IH_T(x)dx}{\int_{-\infty}^{+\infty} IH_T(x)dx} = \frac{\int_{-\infty}^{v} IH_{ET}(x)dx}{\int_{-\infty}^{+\infty} IH_{ET}(x)dx} \tag{16}$$

An important aspect of the proposed method is that Eq. 6 produces the same probability value $P(t|\mathbf{p}, r, \mathbf{q})$, regardless of the observation model template $\mathbf{P}(v|m)$ used:

Theorem 2.3 *Let $P(t|\mathbf{p}, r, \mathbf{q})$ be the likelihood of matching intensity t at position $\mathbf{p}$ to intensity r at position $\mathbf{q}$, computed based on observation model template $\mathbf{P}(v|m)$. Let also $\hat{P}(t|\mathbf{p}, r, \mathbf{q})$ be the likelihood of matching intensity t at position $\mathbf{p}$ to intensity r at position $\mathbf{q}$, computed based on observation model template $\hat{\mathbf{P}}(\hat{v}|m)$. Then, for any $\mathbf{P}(v|m)$ and $\hat{\mathbf{P}}(\hat{v}|m)$, $P(t|\mathbf{p}, r, \mathbf{q}) = \hat{P}(t|\mathbf{p}, r, \mathbf{q})$.*

PROOF — *Applying the definition of $P(t|\mathbf{p}, r, \mathbf{q})$ stated in Eq. 6, the theorem is true if*

$$\begin{aligned}
&\alpha \int_{-\infty}^{+\infty} \exp\left(-\frac{(t-\mu_{T\mathbf{p}v})^2}{2\sigma_T^2}\right) \exp\left(-\frac{(r-\mu_{R\mathbf{q}v})^2}{2\sigma_R^2}\right) \\
&\int_{-\infty}^{+\infty} P(v|m)P(m)dmdv = \\
&\alpha \int_{-\infty}^{+\infty} \exp\left(-\frac{(t-\hat{\mu}_{T\mathbf{p}\hat{v}})^2}{2\sigma_T^2}\right) \exp\left(-\frac{(r-\hat{\mu}_{R\mathbf{q}\hat{v}})^2}{2\sigma_R^2}\right) \\
&\int_{-\infty}^{+\infty} \hat{P}(\hat{v}|m)P(m)dmd\hat{v},
\end{aligned} \tag{17}$$

where $\mu_{T\mathbf{p}v}$ and $\mu_{R\mathbf{q}v}$ are the resulting mean values of matching the expected histograms IH_{ET} and IH_{ER}, computed based on observation model template $\mathbf{P}(v|m)$, to IH_T and IH_R, respectively. In a similar way, $\hat{\mu}_{T\mathbf{p}\hat{v}}$ and $\hat{\mu}_{R\mathbf{q}\hat{v}}$ are the resulting mean values of matching the expected histograms $IH_{\hat{E}T}$ and $IH_{\hat{E}R}$, computed based on observation model template $\hat{\mathbf{P}}(\hat{v}|m)$, to IH_T and IH_R, respectively. The relationship between the intensity domains v and $\hat{v}$ can be better understood with the aid of Fig. 2. The computation of the corresponding intensities among the observation model template, the expected intensity histogram and the image intensity histogram is done by matching cumulative areas. Based on the observation model template $\mathbf{P}(v|m)$, the probability distribution for intensities, $P(v)$, can be computed as

$$P(v) = \int_{-\infty}^{+\infty} P(v|m)P(m)dm. \tag{18}$$

The same can be done for the observation model template $\hat{\mathbf{P}}(\hat{v}|m)$:

$$\hat{P}(\hat{v}) = \int_{-\infty}^{+\infty} \hat{P}(\hat{v}|m)P(m)dm. \tag{19}$$

The probability functions describing the atlases are continuous, so the cumulative area function $C_V(v)$, defined as

$$C_V(v) = \int_{-\infty}^{v} P(x)dx, \tag{20}$$

is also continuous and monotonic. The cumulative function $C_{\hat{V}}(\hat{v})$ for $\hat{P}(\hat{v})$ can be defined in a similar way. It follows that, since both $C_V(v)$ and $C_{\hat{V}}(\hat{v})$ are continuous monotonic and the areas bellow $P(v)$ and $\hat{P}(\hat{v})$ equal to unity, for each area $C_V(v)$ there will be a corresponding area value for $C_{\hat{V}}(\hat{v})$.

In order to proceed with the histogram matching, let us define the cumulative function for the other histograms depicted in Fig. 2, IH_{ET}, IH_T, IH_{ER}, IH_R, $IH_{\hat{E}T}$ and $IH_{\hat{E}R}$, which will be denoted C_{ET}, C_T, C_{ER}, C_R, $C_{\hat{E}T}$ and $C_{\hat{E}R}$, respectively. From the equality of areas shown in Fig. 2, it follows that

$$C_T(\mu_{T\mathbf{p}v}) = C_{ET}(v_{ET}) = C_V(v) = C_{ER}(v_{ER}) = C_R(\mu_{R\mathbf{q}v}) = C_T(\hat{\mu}_{T\mathbf{p}\hat{v}}) = C_{\hat{E}T}(\hat{v}_{\hat{E}T}) = C_{\hat{V}}(\hat{v}) = C_{\hat{E}R}(\hat{v}_{\hat{E}R}) = C_R(\hat{\mu}_{R\mathbf{q}\hat{v}}). \quad (21)$$

Now, consider the inverse of the cumulative function which, given a cumulative area, finds the corresponding intensity in the histogram. Based on the relationship stated in Eq. 21, we have that

$$\begin{aligned} \mu_{T\mathbf{p}v} &= C_T^{-1}(C_V(v)), \\ \hat{\mu}_{T\mathbf{p}\hat{v}} &= C_T^{-1}(C_{\hat{V}}(\hat{v})), \\ \mu_{R\mathbf{q}v} &= C_R^{-1}(C_V(v)), \\ \hat{\mu}_{R\mathbf{q}\hat{v}} &= C_R^{-1}(C_{\hat{V}}(\hat{v})). \end{aligned} \quad (22)$$

The cumulative function of a histogram has the property that its derivative is the original histogram. Applying this property to C_V and $C_{\hat{V}}$, we have that

$$dC_V(v) = P(v)dv \quad and \quad dC_{\hat{V}}(\hat{v}) = \hat{P}(\hat{v})d\hat{v}. \quad (23)$$

From Eq. 18, 19, 22 and 23, the integration variables of Eq. 17 can be changed from v to $C_V(v)$ and from $\hat{v}$ to $C_{\hat{V}}(\hat{v})$, resulting on

$$\alpha \int_0^1 \exp\left(-\frac{(t - C_T^{-1}(C_V(v)))^2}{2\sigma_T^2}\right) \exp\left(-\frac{(r - C_R^{-1}(C_V(v)))^2}{2\sigma_R^2}\right) \frac{\int_{-\infty}^{+\infty} P(v|m)P(m)dm}{\int_{-\infty}^{+\infty} P(v|m)P(m)dm} dC_V(v) =$$

$$\alpha \int_0^1 \exp\left(-\frac{(t - C_T^{-1}(C_{\hat{V}}(\hat{v})))^2}{2\sigma_T^2}\right) \exp\left(-\frac{(r - C_R^{-1}(C_{\hat{V}}(\hat{v})))^2}{2\sigma_R^2}\right) \frac{\int_{-\infty}^{+\infty} \hat{P}(\hat{v}|m)P(m)dm}{\int_{-\infty}^{+\infty} \hat{P}(\hat{v}|m)P(m)dm} dC_{\hat{V}}(\hat{v}). \quad (24)$$

The inner integrals can be canceled. From Eq. 21, we have that $C_V(v) = C_{\hat{V}}(\hat{v})$, leaving identical the right and left hand sides of Eq. 24.

3 Results

The likelihood model was compared to the cross-correlation and mutual information metrics in a set of 1624 experiments in which controlled synthetic deformations and position-dependent low-frequency artifacts were applied to the Harvard Atlas — a labeled brain scan of a white, 25-year-old, right-handed male (see [12] for details about the dataset). The effectiveness of matching for each similarity measure was quantitatively evaluated based on the mean squared deformation error, computed from the resulting displacement field $\mathbf{u}$ and the original synthetic deformation $\mathbf{s}$ applied to the data:

$$MSDE(\mathbf{u}, \mathbf{s}) = \frac{1}{n}\sum_{\mathbf{p}} |\mathbf{s}(\mathbf{p}) + \mathbf{u}(\mathbf{p} + \mathbf{s}(\mathbf{p}))|^2,$$

where $|\ |$ denotes the vector magnitude and n is the number of voxels in the image. The error is measured in square pixels.

The set of experiments comprised two steps: the generation of input files and image registration. The warping algorithm used to deform the reference image to match the test images is based on the elastic matching model and implemented in a multiresolution way [2, 6]. The input files required for matching are the reference and test images at each resolution level, grid files describing the mesh of finite elements and elastic properties of the media. In our multiresolution elastic matching experiments, the images were matched in 5 different levels of resolution and the results obtained at a coarse level were used as the first approximation to the next finer level. No global registration was required in this set of experiments, since the slices were already rigidly aligned.

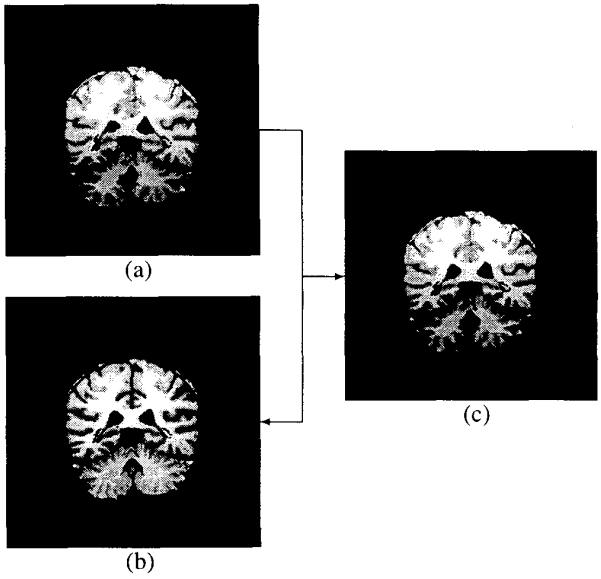

Figure 3: Deformed image (c) obtained by matching slice 48 of the Harvard Atlas (b) to its noisy deformed version (a), using likelihood models.

The results for one of the 1624 experiments of image registration based on likelihood models, in which both spatial and intensity distortions were applied is shown in Fig. 3. The mean squared deformation error obtained for this experiment was equal to 2.37 squared pixels. The same registration experiment based on the cross-correlation and mutual information similarity metrics resulted on errors of 2.57 and 5.19, respectively. For the global and local histogram matching methods, the obtained error were respectively 5.26 and 3.33. For the whole set of experiments, the average error obtained with the cross-correlation was

19.75% larger than the one obtained with the likelihood model metric. The difference between the results obtained with cross-correlation and likelihood models is progressively more substantial as larger deformations are applied. The results obtained with mutual information exemplifies the method's inability to handle local deformations. For the whole set of experiments, the average error was 94% larger than the obtained with the likelihood measure. In all cases, the error was proportional to the amount of deformation imposed by the synthetic distortions, whereas it did not vary much as a function of the synthetic intensity distortion or the anatomy. Indeed, all the measures proved to be reasonably stable with respect to the particular slice used for matching.

The variance of the mean squared deformation error also deserves attention. It can be interpreted as a measure of instability of a given measure with respect to changes in the imaged anatomy, amount of deformation and artifacts. Whereas the mean error is a measure of effectiveness, the variance may reflect robustness. When considering the whole dataset, the variance for the cross-correlation was 70.91% larger than the one obtained for the likelihood models.

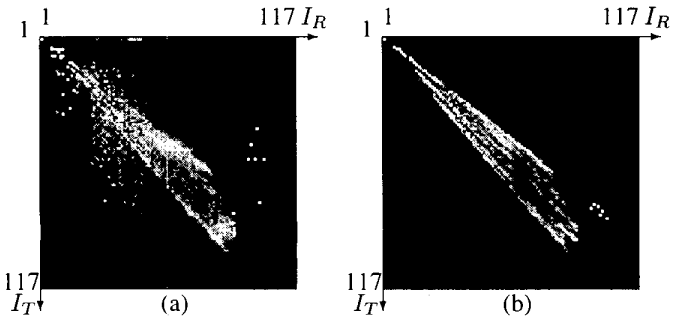

Figure 4: Joint probability histogram obtained for image registration with likelihood models, intensity and spatial distortion (a). The joint probability histogram obtained from rigid registration without spatial distortion is also shown (b).

The relationship between the intensities in the reference and test images can be observed if we plot a global joint histogram that graphically shows the probability of mapping intensity r of the reference to intensity t of the test image. This distribution, denoted by $P(t|r)$, may provide information about artifacts in the image, which causes a given intensity r to be assigned to more than one intensity t, with equally high probability. Fig. 4 shows the joint histogram computed based on the resulting displacement field of the experiment depicted in Fig. 3. It can be compared to the joint histogram generated by rigidly matching the original image to its noisy version (without spatial distortion), which provides a good reference for the true distribution. Probabilities are displayed in logarithmic scale, in order to enhance the visualization of details in the distribution. Intensities are normalized so that, for each column, the largest probability value is shown as white. It can be seen that the likelihood-based method provides a good approximation for the distribution, which corroborates to its effectiveness and partially explains the superior results obtained in the experiments on image registration.

4 Conclusion

In this work, we have presented a discussion of similarity measures used for image registration. Similarity measures are essential to the image warping process, since they represent the external forces that are applied to the reference image, in order to produce a warped version that matches the test image. A poor model of the intensity mapping between a pair of images to be matched using intensity-based measures can result in incorrect registrations and impact morphological analyses. The main objective of this work was to develop a computational tool that provides accurate data to support subsequent analysis of anatomical deformations and pathologies.

A novel algorithm was presented, which estimates a probability density function based on prior information about the sensors used in image acquisition. It implements a Bayesian approach to density estimation which is both efficient with respect to computational cost and robust to artifacts. In the discrete implementation, the method requires a labeled volume for each scanner, from which the likelihood models are constructed once and used together with the elastic matching algorithm for subsequent registration of images acquired with the same sensors.

The proposed measures were evaluated and compared to other well-known similarity metrics based on the analysis of effectiveness and robustness. The effectiveness and robustness of a similarity metrics may be reduced when the images to be matched exhibit strong spatial or intensity distortions. While the robustness of the cross-correlation, mutual information and histogram-matching approaches are proven to be restricted to constant noise, likelihood models extend robustness to the class of generic noise.

The application of synthetic spatial and intensity distortions provided a basis for comparison. Instead of a few manually-chosen landmarks, the evaluation of matching was applied to full resulting displacement fields. Effectiveness was analyzed based on a set of qualitative and quantitative evaluation procedures. Quantitative evaluation is achieved by computing the mean squared deformation error, which numerically compares the resulting displacement field with the synthetic spatial distortion applied to the test images.

A set of 1624 experiments with different images, synthetic spatial and intensity distortions was conducted. The average mean squared deformation error obtained with the cross-correlation measure was about 20% larger than the one obtained with the likelihood model metric. Moreover, difference between the results obtained with cross-correlation and likelihood models was progressively more substantial as larger deformations were applied, showing that similarity prior models should be considered important sources of information to improve the results of image matching and provide quality data to further analysis.

References

[1] R. Bajcsy and C. Broit. Matching of deformed images. In *VI International Conference on Pattern Recognition*, pages 351–353. 1982.

[2] R. Bajcsy and S. Kovacic. Multiresolution elastic matching. *Computer Vision, Graphics and Image Processing*, 46:1–21, 1989.

[3] C. Broit. *Optimal registration of deformed images*. PhD thesis, University of Pennsylvania, 1981.

[4] M. A. Brown and R. C. Semelka. *MRI Basic Principles and Applications*. Wiley-Liss, 1995.

[5] J. C. Gee. On matching brain volumes. *Pattern Recognition*, 32:99–111, 1999.

[6] J. C. Gee and D. Haynor. Numerical methods for high-dimensional warps. In A. Toga, editor, *Brain Warping*. Academic Press, San Diego, 1999.

[7] A. Machado. *Likelihood Models for image registration*. PhD thesis, Federal University of Minas Gerais, 1999.

[8] A. Machado, J. C. Gee, and M. Campos. Density estimation for mr image elastic matching. In *Proceedings of the International Symposium on Computer Graphics, Image Processing and Vision*, Rio de Janeiro, 1998.

[9] F. Maes, A. Collignon, D. Vandermeulen, G. Marchal, and P. Suetens. Multimodality Image Registration by Maximization of Mutual Information. *IEEE Trans. Med. Imag.*, 16(2):187–198, 1997.

[10] J. Maintz, E. Meijering, and M. Viergever. General Multimodal Elastic Registration Based on Mutual Information. In *Proceedings of the SPIE Medical Imaging 1998: Image Processing*, San Diego, 1998. Bellingham.

[11] J. Pearl. *Probabilistic Reasoning in Intelligent Systems: Networks of Plausible Inference*. Morgan Kaufman, 1991.

[12] M. Shenton, R. Kikinis, F. Jolesz, S. Pollak, M. LeMay, C. Wible, H. Hokama, J. Martin, D. Metcalf, M. Coleman, and R. McCarley. Abnormalities of the left temporal lobe and thought disorder in schizophrenia: A quantitative magnetic resonance imaging study. *N. Eng. J. Med.*, 327:604–612, 1992.

[13] B. Silverman. *Density estimation for statistics and data analysis*. Chapman & Hall, 1986.

[14] P. Viola. Alignment by Maximization of Mutual Information. *International Journal of Computer Vision*, 24(2):137–154, 1997.